Gravitational Lens Optics

R. D. BLANDFORD, C. S. KOCHANEK, ISRAEL KOVNER, RAMESH NARAYAN

Several instances of multiple imaging of cosmologically distant sources by intervening galaxies and galaxy clusters have been discovered over the past decade. These "gravitational lenses" have distinctive optical properties. Point-like sources such as quasars generally produce two or four images when lensed, whereas extended sources such as galaxies produce spectacular arcs and rings. The salient features of most of the observations can be reproduced with the use of simple elliptical lens models that approximate the lenses made by ellipsoidal mass distributions such as are common in the universe. In addition to illustrating simple optics in operation on a cosmological scale, multiple images and arcs provide useful probes of the lensing galaxies and clusters. Also, gravitational lenses can make magnified images of cosmologically distant sources and may eventually furnish important cosmographic data such as the Hubble constant.

THE IDEA THAT LIGHT RAYS CAN BE BENT BY THE FORCE OF gravity goes back to Newton's *Opticks*. However, it was Einstein who used his general theory of relativity to give the correct expression for the deflection angle α due to a point mass, M, namely,

$$\alpha = 2\int \mathbf{g}_\perp dt/c = 4GM/bc^2 \quad (1)$$

where $\mathbf{g}_\perp$ is the perpendicular component of the gravitational acceleration, G is the gravitational constant, c is the speed of light, and b is the impact parameter, the lateral offset of the ray from the mass. This formula, valid for small angles, is twice the Newtonian expression. The measurement of the predicted deflection of the positions of stars due to the sun ($\sim 1.8''$ at the limb) during a solar eclipse in 1919 provided a notable success for general relativity and made Einstein into a household name.

Over the past decade, astronomers have discovered over a dozen examples of cosmologically distant objects that have been multiply imaged by intervening mass. In this review, we describe the properties of gravitational lenses and explain how generic elliptical lenses can reproduce many of the observed characteristics of the images (*1–3*).

Multiply Imaged Quasars

After 60 years of waiting, astronomers discovered an even more spectacular example of gravitational deflection than that caused by the sun when they found a multiply imaged quasar in 1979 (*1*). (A quasar is an active nucleus of a galaxy that outshines the surrounding stars and for our purposes can be regarded as a point source. Most quasars are at cosmological distances.) This quasar, known as Q0957 + 561 (Fig. 1), was found to consist of two images separated by 6 arc seconds on opposite sides of a giant foreground galaxy. The optical spectra of the two images were identical, although the fluxes differed, just what one would expect for an intervening lens. Subsequent observations at radio wavelengths confirmed this diagnosis.

Further examples of multiple imaging soon followed (Fig. 2) (*3*). Q1115 + 080 is a bright quasar exhibiting four images. Q2016 + 112, one of the more distant quasars with a redshift (a measure of distance) of 3.3, was discovered in a radio survey. In this case, there are three images at the vertices of a right angle triangle. Q2237 + 0305 was a big surprise with a high redshift quasar located at the center of a nearby spiral galaxy. Some astronomers thought that this was a demonstration that redshifts do not measure distance. However, subsequent observations revealed four images of the quasar, verifying that the quasar does indeed lie behind the galaxy. A fifth example is Q0142 + 100, which is distinctive in having two images with very different fluxes. Roughly four more convincing examples of multiple imaging are known, and there are many more objects for which this is suspected. Deciding which objects exhibit multiple imaging is frequently controversial. Many criteria, such as similarity of optical spectra, have turned out to be unreliable and must be supplemented with additional evidence before we can conclude that two images derive from the same source (*2*).

Gravitational Lenses

The optical arrangement is quite simple, involving a source S (usually a distant quasar or galaxy), a lens L (either a galaxy or a cluster of galaxies), and the observer O (that is, us), but it differs in two important ways from conventional laboratory optics (Fig. 3). First, in man-made lenses there is usually a linear dependence between the deflection angle and the distance of the ray from the optic axis. Consequently, there is a unique ray connecting a point source to each point in the observer plane (except at foci). In contrast, gravitational lenses are nonlinear, and there can be more than one ray connecting a source to the observer. This leads to multiple images, just as waves on the surface of the ocean can form multiple images of the setting sun. Second, in laboratory optics it is common to have a fixed point source and to move the point of observation. In gravitational lenses, the observer is effectively fixed but we look at a variety of different sources.

R. D. Blandford and C. S. Kochanek are in the Department of Theoretical Astrophysics, California Institute of Technology, Pasadena, CA 91125. I. Kovner is in the Physics Department, Weizmann Institute, Rehovot 76100, Israel. R. Narayan is at Steward Observatory, University of Arizona, Tucson, AZ 85721.

Deflection angles in gravitational lenses are typically smaller than a minute of arc, and the small angle approximation is adequate. We trace rays backwards from O and denote the angular positions of sources and images on the sky by two vectors **s** and **r** lying in the source plane and image plane, respectively. The image-to-source mapping by a thin gravitational lens is then given by the equation

$$\mathbf{r} \rightarrow \mathbf{s}: \mathbf{s} = \mathbf{r} - \frac{D_{LS}}{D_{OS}}\alpha(\mathbf{r}) \qquad (2)$$

The "angular diameter" distances D_{ij}, where i, j = S, L, O, are defined for a particular cosmological model as the ratio of the linear size of a source to its observed angular size (Fig. 3b).

The total deflection angle α is the vector superposition of the deflections due to all the mass elements in the lens. We can therefore use Eq. 1 if we treat $\mathbf{g}_\perp$ as the total Newtonian gravitational acceleration perpendicular to the line of sight. The integral $\int \mathbf{g}_\perp cdt$ can, in turn, be expressed as the two-dimensional gradient of the two-dimensional Newtonian potential $\phi^{(2)}$. We may introduce a scaled potential Φ, defined by

$$\frac{D_{LS}}{D_{OS}}\alpha = \nabla\Phi = \frac{2D_{LS}}{D_{OL}D_{OS}c^2}\nabla\phi^{(2)} \qquad (3)$$

This potential satisfies the two-dimensional Poisson equation, $\nabla^2\Phi = 2\Sigma/\Sigma_{crit}$, where $\Sigma(\mathbf{r})$ is the surface density in the lens and $\Sigma_{crit} = c^2D_{OS}/4\pi GD_{OL}D_{LS}$ is known as the critical density. A sufficient (though not necessary) condition for multiple imaging (of a suitably placed source) is that Σ should exceed Σ_{crit} ($\sim$1 g cm^{-2} for cosmologically distant sources and lenses) somewhere within the lens.

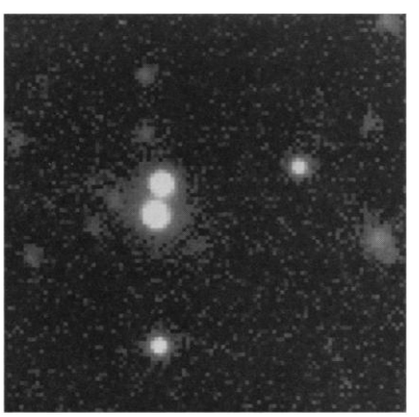

Fig. 1. Photograph of the first multiply imaged quasar discovered, Q0957 + 561. The two bright images in the center are the A and B images of a single background quasar. These images appear superposed on a fainter nebulosity, which is an intervening giant galaxy. The extended faint images in the field are smaller galaxies belonging to the same cluster. All the galaxies contribute to the gravitational lens. (Image prepared by E. Falco and R. Schild.)

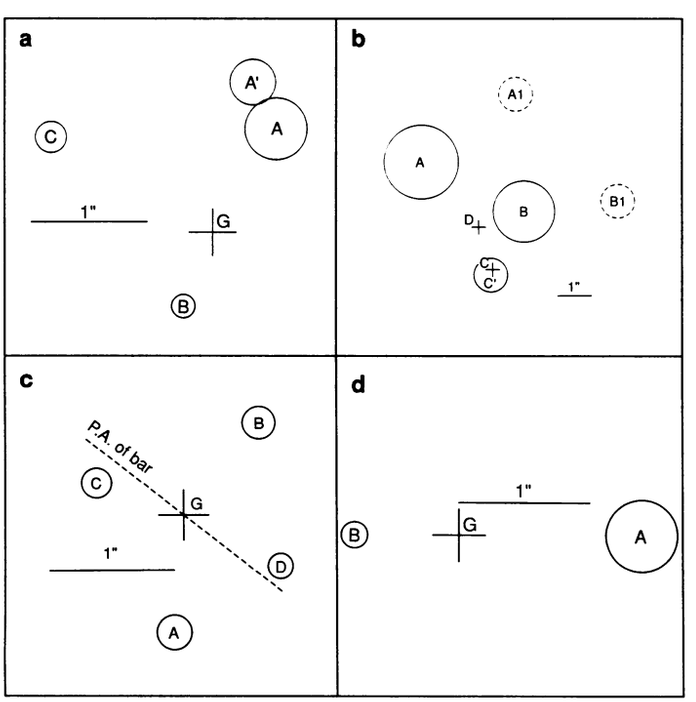

Fig. 2. Image locations and magnifications (represented by the sizes of the circles) for four gravitationally lensed quasars referred to in the text. The lensing galaxy, where observed, is indicated by a cross. (**a**) Q1115 + 080, (**b**) Q2016 + 112, (**c**) Q2237 + 0305, and (**d**) Q0142 + 100. In (c) the position angle (P.A.) of the bar in the lensing galaxy is shown.

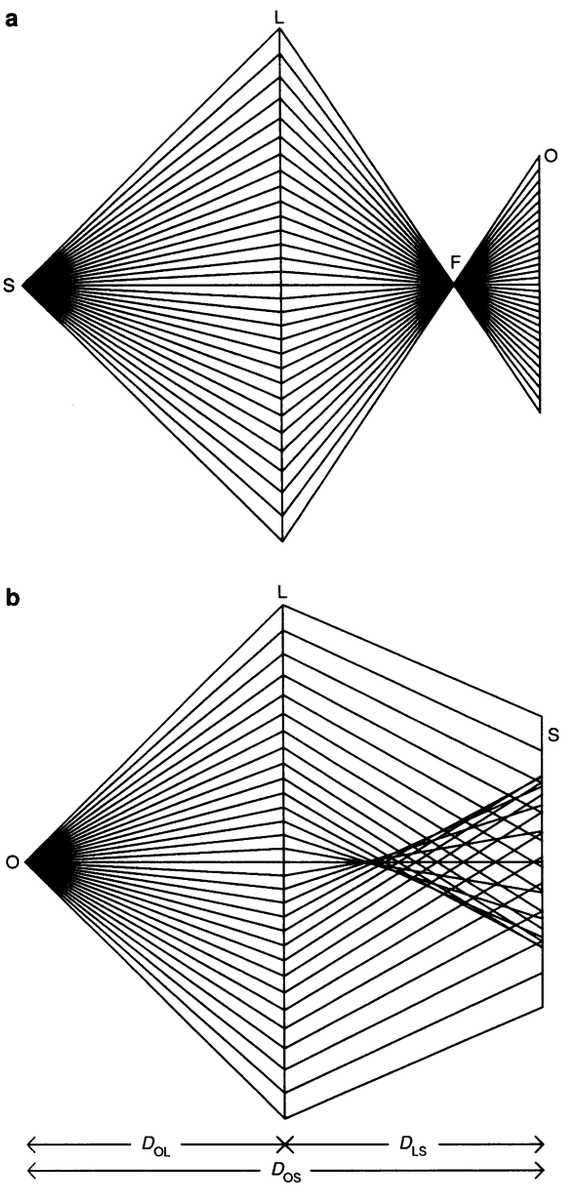

Fig. 3. Schematic representation of the difference between a linear laboratory lens and a nonlinear gravitational lens. (**a**) Linear lens. Light from a source S passes by a single lens L, where it suffers a deflection proportional to its displacement, and then passes through a focus F on its way to an observer O. Only one ray connects S to O in general. (**b**) Nonlinear gravitational lens, showing rays emanating backwards from a fixed observer O. As the deflection by the lens L depends nonlinearly on the displacement, the focus F (now on the source side of the lens) unfolds to form a cusp caustic. When a source S is located beyond the cusp, three rays connect it to the observer and three images are seen.

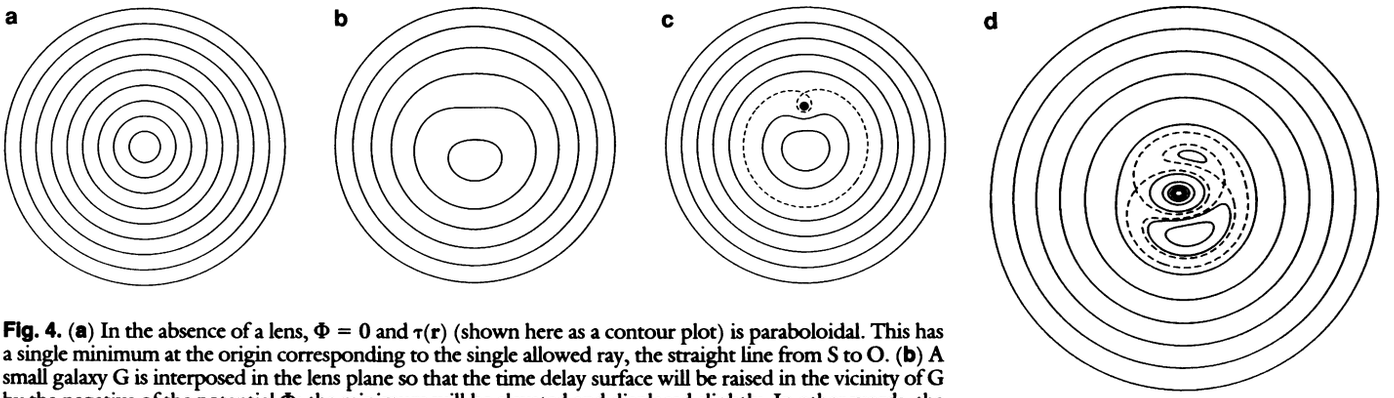

Fig. 4. (**a**) In the absence of a lens, $\Phi = 0$ and $\tau(\mathbf{r})$ (shown here as a contour plot) is paraboloidal. This has a single minimum at the origin corresponding to the single allowed ray, the straight line from S to O. (**b**) A small galaxy G is interposed in the lens plane so that the time delay surface will be raised in the vicinity of G by the negative of the potential Φ; the minimum will be elevated and displaced slightly. In other words, the ray will be deflected slightly by the galaxy and the total travel time along the ray will be increased. (**c**) A large mass is interposed, and the time delay surface will be raised so much that extra stationary points (images) are created at a maximum and a saddle point of the surface. (**d**) If the mass has an elliptical distribution of surface density, then five images can be created.

Fermat's principle. A particularly helpful way to understand multiple imaging is to rewrite the vector equation (Eq. 2) as an action principle by defining an arrival time delay, in scaled units of $D_{OL}D_{OS}/cD_{LS}$, by (*4*)

$$\tau(\mathbf{r}) = 1/2(\mathbf{r} - \mathbf{s})^2 - \Phi(\mathbf{r}) \qquad (4)$$

This time delay is proportional to the extra time involved when light travels along a straight line from S to a point marked with coordinates $\mathbf{r}$ in the lens plane and then in a straight line to us at O rather than in a straight line directly from S to O. The first term on the right in Eq. 4 is an approximation to the extra path length, calculable with the Pythagorean theorem. The second term is a general relativistic time delay whose effect has been measured directly in the solar system by means of interplanetary radar experiments. [We can mimic this effect by pretending that spacetime is flat and introducing a "gravitational refractive index," $n = 1 - 2\phi^{(3)}/c^2$, where $\phi^{(3)}$ is the three-dimensional Newtonian potential.]

In terms of τ, Eq. 2 is simply $\nabla\tau = 0$. This is an illustration of Fermat's principle, which states that of all possible null paths from S to O, the actual paths followed by the light are those for which the travel time is stationary with respect to infinitesimal changes in the path.

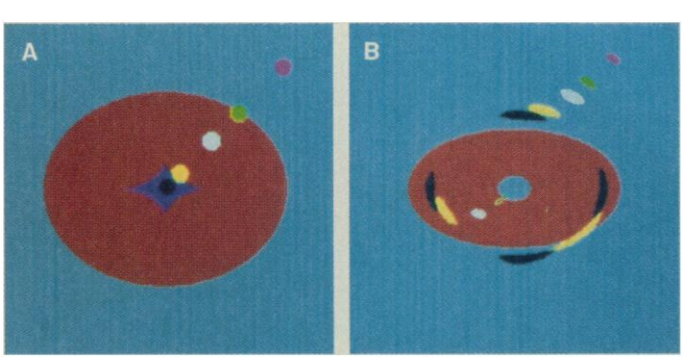

Fig. 5. (**A**) A sequence of source positions in the source plane, starting at the center of an elliptical lens and moving outward along a direction making an angle of 45° to the major axis. The region in the source plane where five images are created is colored dark blue. It is bounded by a four-cusped inner caustic associated with tangentially merging images. The three-image region is colored red and is bounded by the outer caustic associated with radially merging images. (**B**) Image positions corresponding to (a) coded by the colors of the associated sources. (Note that we are strictly assuming that the source is infinitesimally small.) The image shapes exhibit the magnifications induced by the lens and are to scale. The inner gray-red boundary is the radial critical curve where merging images produced by sources located on the radial caustic are found. The outer gray-red boundary is the tangential critical curve.

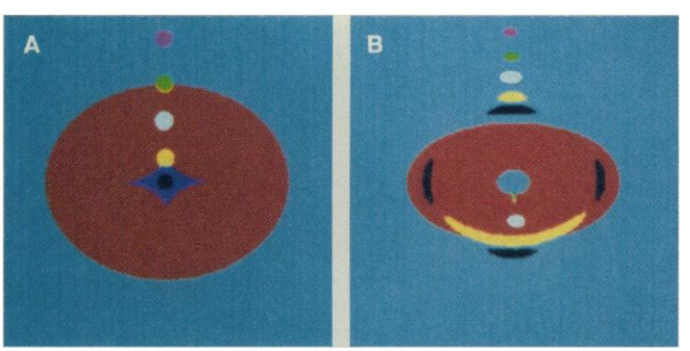

Fig. 6. (**A**) Source positions along the minor axis passing through a cusp caustic. (**B**) Image positions corresponding to (A).

Image location. Consider a plot of the time delay surface $\tau(\mathbf{r})$ (Fig. 4). In the absence of the lens there is a single minimum, and hence a single image, corresponding to the direct ray from S to O. Adding a galaxy along the line of sight modifies the surface, shifts the position of the minimum, and may introduce extra stationary points. For example, in Fig. 4c, there is a maximum very close to the center of the galaxy and a saddle point on the opposite side from the original ray. The positions of these three stationary points are the positions of the three images that we will see. Measuring the image separations allows us to estimate the mass lying between the images and to compare this mass with that determined from other means. The heights of the three stationary points are the time delays experienced by light as it travels along the three rays. This time delay too can be measured if the source is variable. If we allow the lens to become more complicated (for example, Fig. 4d), extra images will be created. However, as long as the lens is transparent and nonsingular, the time delay surface must be smooth, and the extra images must be created in pairs. There will therefore be an odd number of images in total.

Magnification of images. If we imagine moving a point source slightly, then the point images must also move. Using Eqs. 2 and 4, we see that this is basically the same as shifting the center of the paraboloid given by the first term to the right in Eq. 4. In effect, we can rock the time delay surface through a very small angle, and so the distance that an image will move is governed by the curvature in the time delay surface. If the surface is quite flat, then the image will be displaced a long way, much farther than the distance moved by

the source point. Conversely, if the surface is highly curved, the displacement is small. Now suppose that the source has a finite, though small, size. Because the intensity, that is, the flux of light per unit solid angle, is preserved by a lens, the magnification of the flux from the source is just proportional to the ratio of the angular area of the image to the angular area of the source. So, the flatter the time delay surface, the greater the image magnification.

Distortion of images. If the source has resolvable structure, then the distortion of the image can be detected. We can formally relate the image shape to the source shape by defining a transformation matrix,

$$T_{ij} = \frac{\partial s_i}{\partial r_j} \tag{5}$$

(which is symmetric for a thin lens, $T_{ij} = \partial^2\tau/\partial r_i \partial r_j$) so that $\delta\mathbf{s} = \mathbf{T}\delta\mathbf{r}$. (The indices i, j take values 1, 2 and refer to Cartesian axes in the plane of the sky.) We illustrate the use of this matrix with a lens formed by a homogeneous sheet of matter with potential

$$\Phi = \kappa(x^2 + y^2)/2 + \gamma(x^2 - y^2)/2 \tag{6}$$

where the convergence $\kappa = \Sigma/\Sigma_{crit}$ and the shear $\gamma > 0$ are constant. The axes are chosen to diagonalize the second term, which describes a quadrupole moment produced by a nonlocal mass distribution and is a measure of the astigmatism of the lens. Such a lens distorts circles into ellipses (just like drawing a picture on a sheet of rubber and stretching it), the expansion factors along the two axes being the eigenvalues of $\mathbf{T}^{-1}$, namely, $(1 - \kappa + \gamma)^{-1}$ and $(1 - \kappa - \gamma)^{-1}$ (*5*). The image magnification is the Jacobian determinant, $|T^{-1}| = [(1 - \kappa)^2 - \gamma^2]^{-1}$.

For a general lens, the transformation matrix $\mathbf{T}$ varies with position. There can then be lines in the image and source planes where $1 - \kappa = \pm\gamma$. At these locations, which are called critical lines in the image plane and caustics in the source plane, the magnification diverges, corresponding to the image being stretched infinitely along one direction (*6*). Caustics play an important role in our understanding of gravitational lensing.

Single lenses can invert images, that is, change their parity. Consider an image of a point source at a minimum. If the source is displaced, the image will move in the same direction. Therefore, although the image may be magnified and sheared, it will not be inverted. We define an image signature by the signs of the eigenvalues of the transformation matrix. When $1 - \kappa > \gamma$, the image lies at a minimum and has a (+, +) signature. When $1 - \kappa < -\gamma$, the image lies at a maximum, and the image is inverted twice, side over side and top over bottom [signature (−, −)], leaving it rotated through a half turn but with the same parity as the source. An image at a saddle, $-\gamma < 1 - \kappa < \gamma$, will be inverted only once [signature

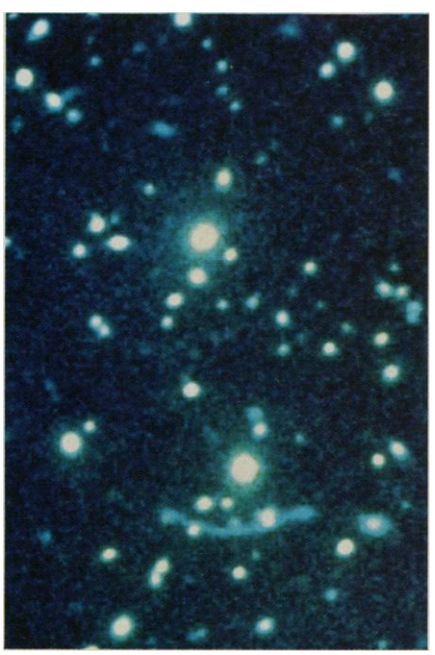

Fig. 7. Deep optical image of the galaxy cluster, A370, showing a prominent blue arc, which is believed to be a gravitationally distorted image of a background galaxy. There are also six smaller features, which may be distorted images of other galaxies. (Image courtesy of R. Lynds and Kitt Peak National Observatory.)

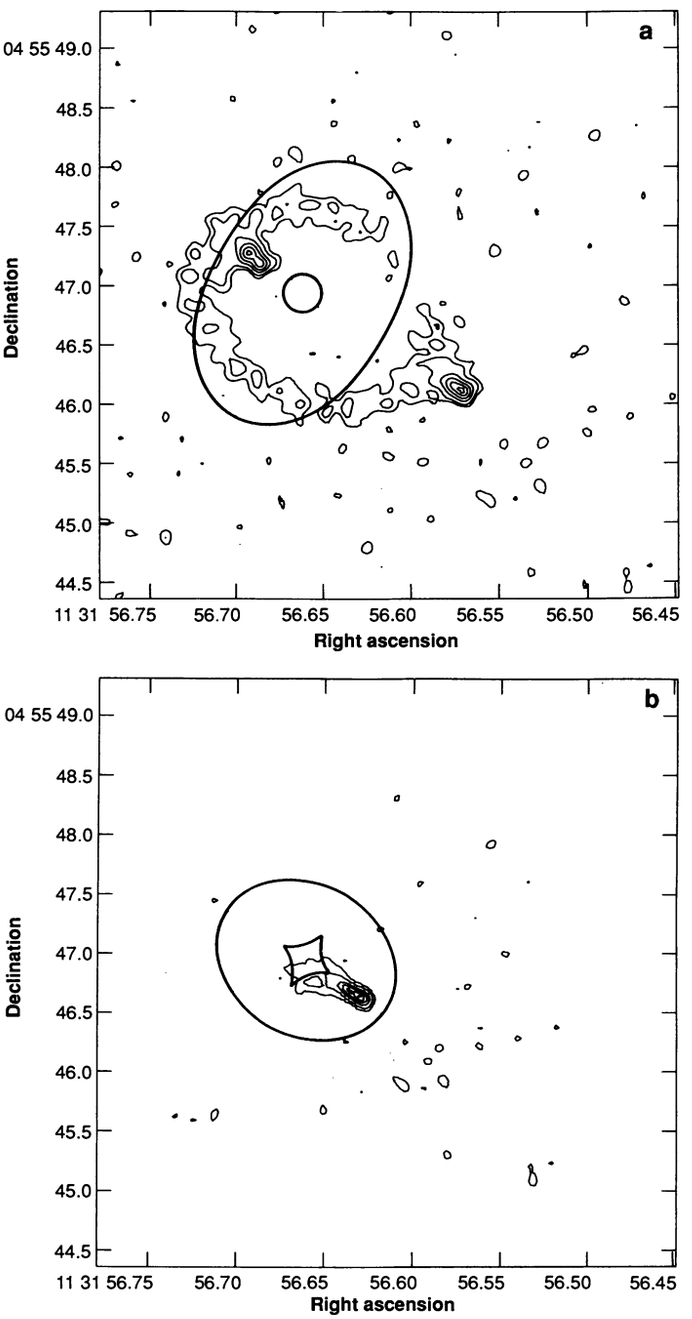

Fig. 8. (**a**) Radio image of the ring source, MG1131 + 0456. A galaxy (not shown) has been found at the center of the ring and is believed to be responsible for distorting the image. (**b**) Reconstruction of the underlying source.

(+, −)], so that it has the opposite parity to the source.

Although we do not determine the transformation matrices **T** of the images directly, we can measure the relative magnifications for unresolved sources. When the sources are resolved, for example, by using the techniques of very long baseline interferometry, transformation matrices between images can also be determined. This has been done for the compact radio structure in Q0957 + 561, and the two images have opposite parity just as expected (*3*). In general, relative magnifications can be used to constrain the imaging geometry when modeling the mass distribution in the lens.

Multiple Imaging by Elliptical Lenses

Most of the observed gravitational lenses fall into two classes:

1) The source is a quasar, and the lens is dominated by a galaxy comprising $\gtrsim 10^{11}$ stars and "dark" matter. The lensing galaxy has been seen in several (but not all) cases.

2) The source is an extended galaxy, and the lens is dominated by a large cluster of galaxies.

In both cases, we expect the mass in the lens to extend well beyond the region of interest for lensing.

When a self-gravitating collection of particles (stars, galaxies) creates multiple images, the image separations are comparable with the individual image deflections, which are given by $\alpha \sim 4\pi\sigma^2/c^2$, where σ is the one-dimensional velocity dispersion in the particles. For stars in a massive galaxy, $\sigma \sim 300$ km s^{-1} and $\alpha \sim 2''$; for galaxies in a rich cluster, $\sigma \sim 1000$ km s^{-1} and $\alpha \sim 20''$. Once the scale difference is factored out, the underlying mass distributions of the two types of lenses are roughly similar and the geometrical arrangements of the images also tend to be qualitatively the same.

Model elliptical potential. A typical gravitational lens model has a surface density variation over radii of interest that decreases approximately as a power law, $\Sigma \propto r^{-1}$, outside a central core region of radius r_c; inside r_c the density deviates from this law and levels off to a finite value at the center of the lens. In addition, the density distribution is usually ellipsoidal, implying an elliptical surface density distribution in projection. These features may be conveniently represented by a simple two-dimensional potential of the form (*7*)

$$\Phi = \Phi_0[1 + (1 - \epsilon)x^2 + (1 + \epsilon)y^2]^{1/2} \qquad (7)$$

where x, y are angular coordinates on the sky, measured in units of r_c and aligned with the principal axes of the potential, and ϵ is the ellipticity responsible for the astigmatism. This model is adequate for the purposes of the present discussion, which concentrates on the qualitative features of multiple imaging, but serious modeling requires more complex potentials representing realistic surface density distributions.

The condition for multiple imaging of a source by a lens described by this potential is that $|\Phi_0| \gtrsim 1$. This condition is amply satisfied by most distant galaxies but may be only marginally satisfied by rich clusters. When $\Phi_0 >> 1$, a strongly deamplified image will generally be formed near the lens center on a highly curved maximum in the time delay surface. This image will generally not be observable, and this explains why we usually only see an even, not an odd, number of images.

Interpretation of the observations. The number and geometrical arrangement of images depend on the position of the source relative to the center of the lens (Fig. 5). When the source is exactly behind the center of an elliptical lens, four images are located symmetrically along the two principal axes, and the faint fifth image (which we ignore) is at the center. If the source is moved by a small amount, the images too will move by small amounts to a less symmetrical configuration (see Fig. 4d). This case is similar to the four-image configuration reported in the gravitational lens system Q2237 + 0305 (*3*).

As the source is moved outward, two of the images approach each other roughly tangentially and become stretched toward each other. The fluxes increase and the images merge and then disappear just as the source crosses the boundary of the five-image region. The system Q1115 + 080 resembles this case, with two very bright, close images and two fainter, more distant images (*3*). The area of source space corresponding to merging images is small, but this is compensated by the enhanced brightness of the images, which makes these configurations relatively easy to find (*8*). The brightening of images as they merge is a manifestation of the fact that the five-image boundary is a caustic, where neighboring rays traced back from O are brought to a focus at the source plane. This type of caustic is called a fold.

If the lens were circular rather than elliptical, the entire five-image zone in the source plane would collapse into a degenerate point at the center and image configurations resembling Q2237 + 0305 or Q1115 + 080 will not be possible. Therefore, the elliptical distortion of the lens is an important ingredient in the explanation of these cases (and of many others below).

When the source in Fig. 5 is located in the three-image region, there are two bright images (and a weak central image that we ignore). The images are typically at different distances from the lens center and are not collinear with it. It is gratifying that these are indeed the characteristics of the first and most famous gravitational lens system, Q0957 + 561 (*3*). (Actually, in this case, the noncircularity is induced mainly by the mass in the background cluster rather

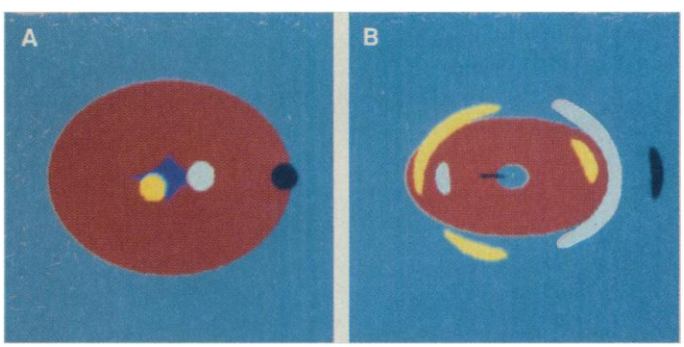

Fig. 9. (**A**) Extended sources (circles) behind an elliptical lens. Arcs are created when the source straddles a caustic, specifically the outer radial caustic (black), a fold portion of the inner tangential caustic (yellow), and a cusp (blue). (**B**) The associated images. The longest arcs are produced when the source covers a cusp in the inner (tangential) caustic. Images associated with the radial caustic are probably not noticeable.

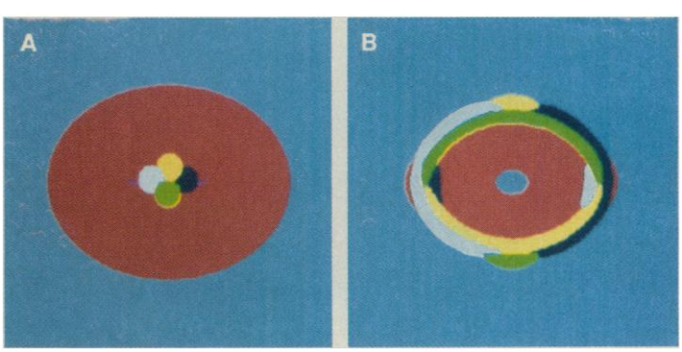

Fig. 10. (**A**) A series of extended sources (circles) that cover most of the inner tangential caustic. (**B**) The associated images that form a complete ring. A source that covers three cusps will make a complete ring.

than in the galaxy. Furthermore, the observed large image separation of 6″ is caused by the magnifying effect of the cluster, which can be modeled by adding a potential of the form used in Eq. 5.)

As the source approaches the outer fold caustic bounding the three- and one-image zones, one of the outer images approaches the central image and the two merge roughly radially. These images tend to be faint because of the small core radius of the lens but are brightened by the effect of the caustic; the net magnification will depend on model details.

Figure 6 shows a second sequence of source positions along one of the symmetry axes of the lens. As the source approaches one of four cusps in the caustic, three of the outer images approach each other, become significantly magnified, and merge into a single image. Even after the source crosses the cusp, the surviving image continues to be bright. Because of the strong magnification, systems in these configurations ought to be easy to find. None of the known cases can be unambiguously identified with this geometry, although Q0142 + 100 may be an example. As the source moves away from the cusp along the symmetry axis, the two images become more nearly equal in magnification and remain collinear with the lens. The compact components A and B in the "Einstein-ring" radio source Q1131 + 0456 probably correspond to this case. A slight shift of the source from the symmetry axis would reproduce the small noncollinearity observed between images and the lens center.

Extended Sources

A major new development in our understanding of gravitational lensing came with the 1986 report of a giant blue luminous arc of light in the central region of a rich cluster of galaxies, A370, at a redshift of 0.37 (Fig. 7). Subsequent observations revealed that the arc redshift is 0.72, thus clearly placing the source behind A370. It is now believed that the arc is the gravitationally lensed image of a galaxy. Similar blue arcs have been discovered in a few other clusters, and several smaller arcs have been found in A370 itself. A related development at radio wavelengths has been the interpretation of a ring-shaped source as the image of an extended radio source by an intervening galaxy (Fig. 8). Another example has just been found (*9*).

The key difference between the multiple quasar images and the arcs and rings is that in the latter case the sources are extended and highly magnified. An extended source can be regarded as a collection of point sources, and the arc (or ring) shape maps the locations of the point images. A study of the point source mappings of Figs. 5 and 6 reveals that elongated images will be produced when the source lies on a caustic. Consider first the simpler outer caustic. When an extended source intersects this, it produces two images, one of which is elongated in a radial direction (Fig. 9). No such case has been identified yet, presumably because the elongation is not particularly striking.

Consider the inner caustic, however. We have seen earlier that each of the four folds of this caustic corresponds to the merging of a pair of outer images. If an extended source happens to intersect one of the folds, it will produce two isolated images and one moderately elongated image. The latter will always be stretched out along a tangential direction with respect to the lens center. If the source intersects two of the folds, for instance, by covering one of the cusps, then a much more highly elongated arc is obtained. Several "giant luminous arcs" have recently been found with tangential elongation (*9*), and these have been interpreted in this way (*10*). When an extended source covers three folds (Fig. 10), all four images merge into a single near-complete ring, with a gap associated with the missed fold. The radio image of Q1131 + 0456 is of this form (*3*).

Giant luminous arcs may become important astrophysical probes (*10*). Because they act like a giant magnifying glass, it might be possible to resolve fine details in the young, blue galaxies that are the sources of most arcs and are not observed locally. They also constrain the shape and depths of cluster potentials directly, without any detailed image analysis. The blue source galaxies are probably in an active stage of star formation, and multiple images of supernovae may be discovered. This would allow us to observe the earliest stages of a supernova and check the self-consistency of the lensing geometry.

Further Possibilities

The foregoing considerations suffice to explain most of the observations to date. However, a variety of other effects have been discussed in the literature.

Galaxy and cluster potentials. Observations of gravitational lenses provide probes of the gravitational potential that are complementary to measurements of velocity dispersion. These may well turn out to be useful in estimating the core radii of clusters and the ellipticity of the central parts of galaxies. Unfortunately, they will probably not provide useful probes of the dark matter surrounding luminous galaxies as this is generally located outside the multiple imaging region.

Singular potentials. Massive black holes probably exist in the nuclei of most galaxies, and it has been suggested that they are present in isolation in the intergalactic medium. They behave like circular lenses with vanishingly small core radii. The images located on the time delay maxima literally vanish. The remaining two images must have opposite parity. Cosmic strings, which are hypothetical topological defects surviving from the earliest moments of the universe, can also deflect rays of light (despite the fact that the surrounding spacetime is flat). They are characterized by an energy per unit length μc^2. A ray making an angle θ with a straight string is deflected through an angle $\alpha = 4\pi\mu\sin\theta$ (*11*). The two images should have similar flux and parity if the string is straight. Cosmic strings should be recognizable through their effects on background galaxies.

Thick lenses. We have restricted our attention to single lenses at a fixed distance. However, two or more separated lenses may be involved (*12*). This seems to be necessary to account for the images seen in Q2016 + 112, where two galaxies are in fact observed. The optics in this case becomes more complicated, and the simple time delay surface exists only in special cases. Some understanding of the most common image arrangements has been obtained from numerical studies.

Microlensing. We have so far treated the lenses as smooth. However, galaxies comprise stars that confer a degree of granularity on the potential. Stars produce a moving caustic network in the source plane. If the source is sufficiently compact (and the continuum-emitting regions of quasars may well be), then many microimages with sizes of order microarc seconds will be created (*13*). As a source crosses a "microcaustic," pairs of microimages will either brighten and then vanish or appear and then fade, and this behavior can be sought.

Quasar statistics. Foreground galaxies can amplify the flux of background quasars without necessarily imaging them multiply. This can modify the inferred distribution of quasar luminosities, a quantity of considerable cosmological interest. Evidence that this is important has come from the recent report that quasars are preferentially found on the sky close to galaxies (*14*). This effect may be found in flux-limited samples of quasars because the gravitational lensing amplification makes the survey slightly deeper behind any intervening galaxies. Some of these quasars may be microlenses and

exhibit flux variability and probe the dark matter in galaxy halos.

Marginal lenses. We have explained how there may be an overrepresentation of sources that are brightened by being close to caustics. A similar bias may be present in favor of marginal lenses that are only just strong enough to create multiple images if the distribution of lens strengths is sufficiently steep (*15*). Marginal lenses generally create three comparably bright images. Many clusters may be marginal.

Hubble constant. If the time delay between two varying images can be measured and the shape of the lens gravitational potential is understood, then we can determine the scaling factor in Eq. 4. This will yield a value for the Hubble constant. Unfortunately, it is not clear that the lenses will be modeled well enough to improve on traditional determinations (*16*). A good test will be to obtain the same value for different sources. It is also possible, although in practice even harder, to determine the mean density of the universe in this way.

Surveys. Many of the foregoing effects are statistical in nature, and unbiased samples of lenses are necessary for proper interpretation. Automated scanning of photographic plates is proving to be an efficient method of finding quasars. In an alternative strategy, the brightest quasars on the sky, some of which are bright as a consequence of gravitational lensing, are being systematically studied for multiple images. The most compact cosmologically distant clusters of galaxies are also being searched for additional arcs and magnified images of background galaxies (*17*).

The study of gravitational lenses has already provided a graphic cosmic demonstration of some elementary ideas from geometrical optics. It is reassuring that most observed phenomena can be accounted for without the need to invoke structures more complex than familiar elliptical mass distributions. It is expected that the number of instances of multiple imaging will increase over the coming years and individual cases will be studied in more detail, particularly with the Hubble Space Telescope (due to be launched this year) and the Very Long Baseline Array (VLBA), a dedicated long baseline radio interferometer currently under construction. Gravitational lensing is becoming a useful approach for probing the galaxy and cluster lenses, magnifying the structure of distant sources, and perhaps also measuring the size of the universe. However, if recent history is any guide, there are many more optical surprises in store.

REFERENCES AND NOTES

1. D. Walsh, R. F. Carswell, R. J. Weymann, *Nature* **279**, 381 (1979).
2. For more detailed reviews of gravitational lenses see: C. R. Canizares, in *Observational Cosmology* [Proceedings of the International Astronomical Union (IAU) Symposium 124], A. Hewitt, G. Burbidge, L.-G. Fang, Eds. (Reidel, Dordrecht, 1987), p. 729; J. R. Gott, in *Dark Matter in the Universe* (Proceedings of IAU Symposium 117), J. Kormendy and G. R. Knapp, Eds. (Reidel, Dordrecht, 1986), p. 219; R. Narayan, in *Quasars* (Proceedings of IAU Symposium 119), G. Swarup and V. K. Kapahi, Eds. (Reidel, Dordrecht, 1986), p. 529; R. D. Blandford and C. S. Kochanek, in *Dark Matter in the Universe* (Proceedings of the Jerusalem Winter School for Theoretical Physics), J. Bahcall, T. Piran, S. Weinberg, Eds. (World Scientific, Singapore, 1987), p. 133. Original references to the theory of gravitational lenses, several of which preceded the observational discovery, are cited in these reviews.
3. R. J. Weymann *et al.*, *Nature* **285**, 641 (1980); C. R. Lawrence *et al.*, *Science* **223**, 46 (1984); J. Huchra *et al.*, *Astron. J.* **90**, 691 (1985); J. N. Hewitt *et al.*, in *Gravitational Lenses*, J. M. Moran, J. N. Hewitt, K.-Y. Lo, Eds. (Springer-Verlag, Berlin, 1989), p. 147.
4. R. Nityananda, unpublished work; P. Schneider, *Astron. Astrophys.* **140**, 119 (1984); R. D. Blandford and R. Narayan, *Astrophys. J.* **310**, 568 (1986); I. Kovner, in preparation.
5. P. J. Young, J. E. Gunn, J. Kristian, J. B. Oke, J. A. Westphal, *Astrophys. J.* **244**, 736 (1981); R. Nityananda and J. P. Ostriker, *J. Astrophys. Astron.* **5**, 235 (1984).
6. K. Chang and S. Refsdal, *Astron. Astrophys.* **132**, 168 (1984); M. V. Berry and C. Upstill, *Prog. Opt.* **18**, 257 (1980); V. I. Arnold, *Catastrophe Theory* (Springer-Verlag, Berlin, 1986).
7. I. Kovner, *Astrophys. J.* **312**, 22 (1987); *ibid.* **316**, 52 (1987); R. D. Blandford and C. S. Kochanek, *ibid.* **321**, 658 (1987).
8. E. L. Turner, J. P. Ostriker, J. R. Gott, *ibid.* **284**, 1 (1984).
9. G. Soucail, B. Fort, Y. Mellier, J. P. Picat, *Astron. Astrophys.* **172**, 414 (1987); R. Lynds and V. Petrosian, *Bull. Am. Astron. Soc.* **18**, 1014 (1987); B. Fort, J. L. Prier, G. Mathez, Y. Mellier, G. Soucail, *Astron. Astrophys.* **200**, 17 (1988); J. N. Hewitt *et al.*, *Nature* **333**, 537 (1988); G. I. Langston *et al.*, *Astron. J.* **97**, 1283 (1989).
10. B. Paczyński, *Nature* **325**, 572 (1987); I. Kovner, in *The Post-Recombination Universe*, North Atlantic Treaty Organization Advanced Study Institutes, N. Kaiser and A. N. Lasenby, Eds. (Kluwer Academic, Dordrecht, 1988), p. 315; S. Refsdal and R. Kayser, *ibid.*, p. 297; S. Grossman and R. Narayan, *Astrophys. J.* **324**, L37 (1988); R. D. Blandford, E. S. Phinney, R. Narayan, *ibid.* **313**, 28 (1987); P. Schneider and A. Weiss, *Astron. Astrophys.* **164**, 237 (1986).
11. B. Paczyński, *Nature* **319**, 567 (1986); A. Vilenkin, *Astrophys. J.* **282**, L51 (1984); J. R. Gott, *ibid.* **288**, 422 (1985).
12. D. Narasimha, K. Subramanian, S. M. Chitre, *Astrophys. J.* **283**, 512 (1984); C. S. Kochanek and J. Apostolakis, *Mon. Not. R. Astron. Soc.* **235**, 1073 (1988).
13. K. Chang and S. Refsdal, *Nature* **282**, 561 (1979); J. R. Gott, *Astrophys. J.* **243**, 140 (1981); P. Schneider and A. Weiss, *Astron. Astrophys.* **171**, 49 (1986); B. Paczyński, *Astrophys. J.* **301**, 503 (1986); B. Greiger, R. Kayser, S. Refsdal, *Astron. Astrophys.* **194**, 54 (1988).
14. R. L. Webster, P. C. Hewitt, M. E. Harding, G. A. Wegner, *Nature* **336**, 358 (1988).
15. I. Kovner, *Astrophys. J.* **321**, 686 (1987).
16. S. Refsdal, *Mon. Not. R. Astron. Soc.* **128**, 307 (1964); P. Gorenstein, E. Falco, I. Shapiro, *Astrophys. J.* **327**, 693 (1988); J. P. Ostriker and M. Vietri, *ibid.* **300**, 68 (1986).
17. R. L. Webster, P. C. Hewett, M. J. Irwin, *Astron. J.* **95**, 19 (1988); J. N. Hewitt *et al.*, in *Gravitational Lenses*, J. M. Moran, J. N. Hewitt, K.-Y. Lo, Eds. (Springer-Verlag, Berlin, 1989), p. 147.

18. R.D.B. and R.N. are indebted to R. Nitayananda for introducing them to the approach described in (*4*) and for invaluable discussion of elliptical lenses. We thank E. Falco and R. Schild for preparing Fig. 1 and R. Lynds for Fig. 7. Supported under NSF grants AST86-15325 and 86-11121, an AT&T Foundation Graduate Fellowship (C.S.K.), and a Sir Charles Close Fellowship (I.K.).

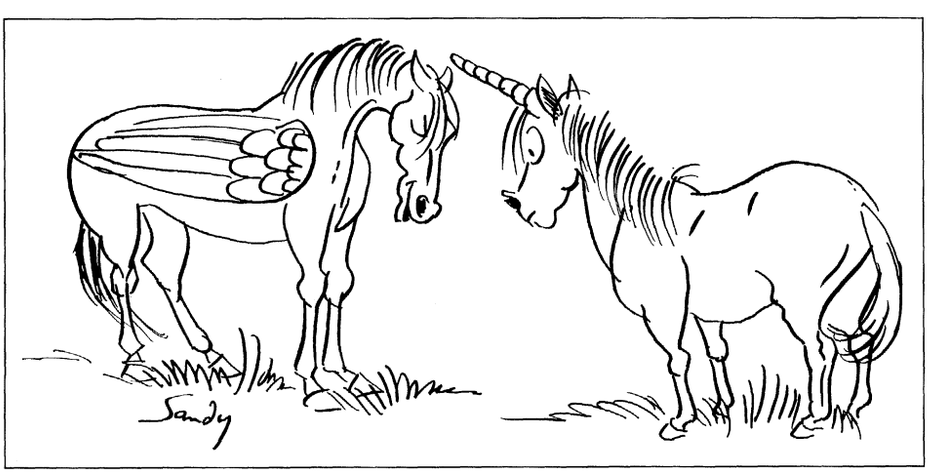

"I hate to brag but, once I was mistaken for Halley's Comet."